Evidence for phase selectivity in excimer-laser-induced amorphization of thermally annealed $Fe_{66}Co_{18}B_{15}Si$ glassy ferromagnet

M. Sorescu
Oklahoma State University, Department of Chemistry, Stillwater, Oklahoma 74078-0447
*and Duquesne University, Bayer School of Natural and Environmental Sciences, Mellon Hall, Pittsburgh, Pennsylvania 15282-1503**

E. T. Knobbe
Oklahoma State University, Department of Chemistry and The University Center for Laser Research, Stillwater, Oklahoma 74078-0447
(Received 15 May 1995)

Pulsed-excimer-laser irradiation effects ($\lambda=308$ nm, $\tau=10$ ns) on the magnetic properties and phase composition of $Fe_{66}Co_{18}B_{15}Si$ metallic glass have been studied by transmission and conversion electron Mössbauer spectroscopy, scanning electron microscopy, and energy-dispersive x-ray analysis. Depending on the number of applied pulses, excimer laser irradiation of amorphous $Fe_{66}Co_{18}B_{15}Si$ was found to induce controlled changes in the magnetic anisotropy without onset of bulk crystallization. Excimer-laser-induced amorphization was observed in partially crystallized $Fe_{66}Co_{18}B_{15}Si$ samples ($T_a=648$ K, $t_a=1$ h) and was found to be accompanied by the development of laser-induced magnetic anisotropy. In completely crystallized $Fe_{66}Co_{18}B_{15}Si$ specimens ($T_a=723$ K, $t_a=1$ h), which contained two crystalline phases of α-(FeCo) and $(FeCo)_3(BSi)$, the effect of excimer-laser-induced amorphization exhibited phase selectivity with respect to the crystalline components of the alloy system. By a combination of complementary methods, the laser-induced phase transformation of thermally annealed $Fe_{66}Co_{18}B_{15}Si$ specimens was shown to consist of partial amorphization and surface oxidation of the irradiated material. When compared to bulk data, a different behavior of the surface magnetic texture and relative abundance of alloy phases was observed. In both as-quenched and excimer-laser-irradiated amorphous $Fe_{66}Co_{18}B_{15}Si$, the hyperfine field $H_{hf}(T)$ exhibited a temperature dependence of $H_{hf}(0)[1-B_{3/2}(T/T_C)^{3/2}]$, indicative of spin-wave excitations. The value $B_{3/2}=0.32\pm0.05$ of the temperature coefficient for the amorphous specimen is twice that obtained for the laser-irradiated $Fe_{66}Co_{18}B_{15}Si$ system. It is concluded that laser-induced quenching stresses reduce the fluctuations of exchange interactions in the irradiated sample. This study suggests that excimer-laser irradiation of glassy ferromagnets offers the intriguing opportunity of designing materials with specific combinations of magnetic and structural properties, not obtainable by conventional methods.

I. INTRODUCTION

The study of structure, magnetic properties, and phase stability of amorphous ferromagnetic alloys has been undertaken as part of developments seeking to elucidate the nature of the microscopic structure-property relationships relevant to rational construction of new magnetic materials. In particular, amorphous iron-cobalt-based alloys have been the subject of intensive theoretical and experimental investigations,[1–7] due to their interesting soft magnetic properties, combined with high permeability and saturation induction over a wide composition range. The larger exchange splitting of Fe is considered a key factor in determining the magnetic behavior of Fe-Co systems.[1]

In order to address the evolution of phases and microstructure in amorphous and nanocrystalline ferromagnetic systems, we have recently proposed a complex methodological approach.[8–11] It relies on the use of pulsed-excimer-laser radiation to study unconventional aspects of materials response by selectively inducing localized changes in the system under investigation. Fundamental effects underlying the interaction of excimer laser radiation with amorphous metals, such as excimer-laser-induced magnetic anisotropy[8] and excimer-laser-induced crystallization,[9] were demonstrated and found to depend on the values of the irradiation parameters and materials properties. The present study has been performed in order to explore the possibility of controlling the magnetic texture and phase equilibrium in amorphous and crystallized Fe-Co based metallic glasses by means of excimer laser irradiation. Due to its local-probe character and the possibility of investigating both bulk and surface characteristics separately, Mössbauer spectroscopy was used to monitor the changes in magnetic anisotropy and phase composition, induced by employing different thermal annealing and laser irradiation treatments. Related morphological changes were examined by scanning electron microscopy (SEM) and resultant crystalline precipitates were characterized by energy-dispersive x-ray analysis (EDX). Excimer-laser-induced amorphization effects were demonstrated in partially and completely crystallized $Fe_{66}Co_{18}B_{15}Si$ samples and found to exhibit selectivity with regard to the crystalline phases in the alloy system. Low-temperature magnetic behavior of amorphous and irradiated $Fe_{66}Co_{18}B_{15}Si$ specimens was studied and conclusions about laser-induced modifications to the fluctuations of exchange interactions are presented.

II. EXPERIMENT

Amorphous alloy $Fe_{66}Co_{18}B_{15}Si$ (Metglas 2605 CO) was supplied by Allied Signal Inc. in the form of 20 μm thick

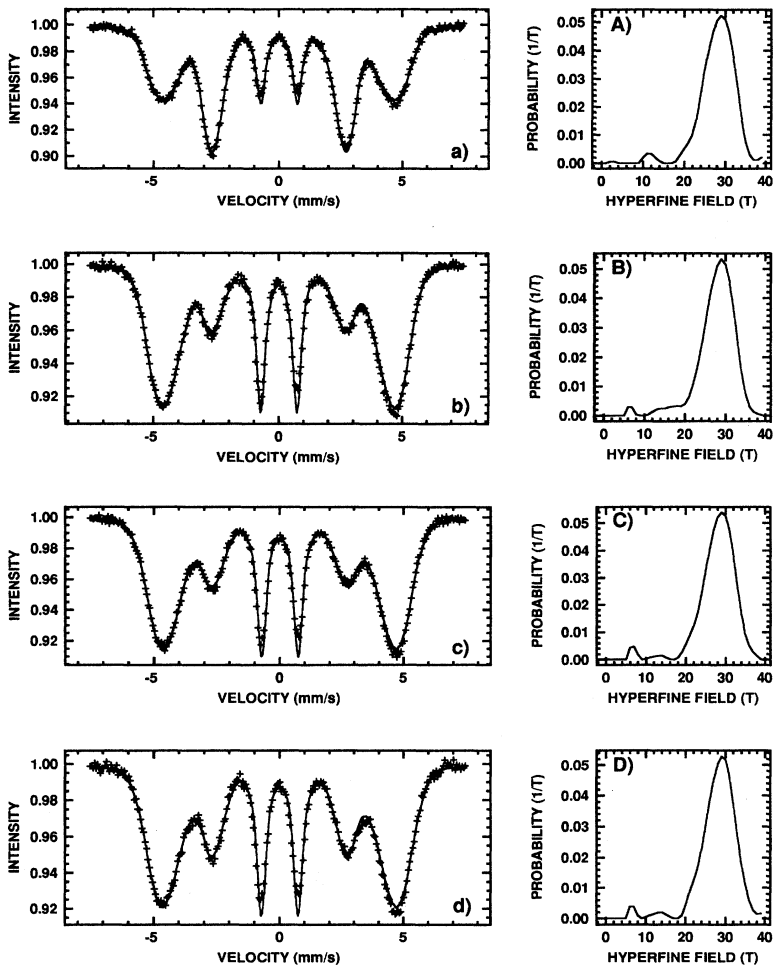

FIG. 1. Room-temperature transmission Mössbauer spectra of the $Fe_{66}Co_{18}B_{15}Si$ samples: (a) in the amorphous as-quenched state and after pulsed-excimer-laser irradiation ($\lambda=308$ nm, $\tau=10$ ns, $\Phi_L=5\times10^{18}$ photons/cm^2, repetition rate 1 Hz) with (b) 2 laser pulses/spot; (c) 5 laser pulses/spot; (d) 10 laser pulses/spot. The hyperfine magnetic field distributions derived from these spectra are shown in (A)–(D). Velocity scale is calibrated relative to α-Fe at 300 K.

ribbons. The material has a Curie temperature $T_C=688$ K, a crystallization temperature $T_x=703$ K, and a magnetostriction constant of 35 ppm. Square samples (2×2 cm) were cut from the foils and exposed on the shiny side to the $\lambda=308$ nm radiation generated by a XeCl excimer laser (Lambda Physik), with the pulse width $\tau=10$ ns, capable of giving an energy $W_p=75$ mJ/pulse. A single-pulse energy density $w=3$ J/cm^2, corresponding to a laser fluence $\Phi_L=5\times10^{18}$ photons/cm^2 was achieved by focusing with a cylindrical fused-silica lens to a spot size of 0.5×5 mm^2. Amorphous samples of $Fe_{66}Co_{18}B_{15}Si$ were irradiated with 2, 5, and 10 laser pulses per spot at a repetition rate of 1 Hz. An acceptable degree of homogeneity was obtained by laser-beam scanning of the sample surface, which was placed on an x-y-z micrometer translation stage.

Partially and completely crystallized $Fe_{66}Co_{18}B_{15}Si$ samples were prepared by annealing the amorphous specimens for $t_a=1$ h at $T_a=648$ and 723 K, respectively. These samples were further exposed to pulsed-excimer-laser irradiation ($\lambda=308$ nm, $\tau=10$ ns, $\Phi_L=5\times10^{18}$ photons/cm^2, $N=2$ laser pulses/spot, repetition rate 1 Hz). All laser treatments were performed in air.

Room-temperature transmission Mössbauer spectra were recorded with the γ ray perpendicular to the ribbon plane using a constant acceleration spectrometer (Ranger Scientific). The 25 mCi γ-ray source was ^{57}Co diffused in Rh matrix, maintained at room temperature. Low-temperature transmission Mössbauer measurements in the temperature range of 15 to 70 K were performed with a closed-cycle refrigerator system (Cryo Industries of America). The sample was mounted in a copper T-style holder and placed in exchange gas. The silicon diode sensor accuracy was better than 0.5 K. Conversion electron Mössbauer spectroscopy (CEMS) spectra of as-annealed and laser-treated surfaces of the metallic samples were collected on the shiny side using a flowing He-CH_4 electron counter.[12] The back-scattered electrons into 2π solid angle were recorded, so that the behavior of surface layers of ~100 nm could be detailed. Least-squares fitting of the Mössbauer spectra corresponding to the amorphous, annealed, and irradiated samples was performed

TABLE I. Relative intensity of lines R_{21}, average hyperfine magnetic field $\langle H_{hf}\rangle$, mean hyperfine field $(H_{hf})_m$, width of the hyperfine magnetic field distribution ΔH_{hf}, and total absorption area in the Mössbauer spectra of the $Fe_{66}Co_{18}B_{15}Si$ system, as a function of the number of applied laser pulses N.

N (laser pulses)	R_{21}	$\langle H_{hf}\rangle$ (kOe)	$(H_{hf})_m$ (kOe)	ΔH_{hf} (kOe)	Resonant area (au)
0	1.10	278.8	283.6	45.1	0.496
2	0.25	276.9	284.5	47.4	0.495
5	0.31	277.8	284.2	49.6	0.513
10	0.39	279.7	285.8	49.7	0.502
Errors:	±0.02	±2.5	±2.5	±2.5	±0.005

with the NORMOS DIST program[13] in the assumption of Lorentzian line shapes. The program uses the constrained Hesse-Rübartsch method to extract the hyperfine field distributions and can analyze superpositions of field distributions and crystalline sites. The relative areas of the outer:inner line pairs of the amorphous component were constrained to the ratio 3:1.

SEM investigations were performed without further surface preparation using a JEOL electron microscope at 25 keV, operating in the secondary-electron-emission mode. Chemical analysis of select microvolumes in the partially crystallized samples was carried out with a Tracor Northern EDX spectrometer. The technique employed was sensitive to chemical elements $Z>11$ and provided an average chemical composition over a volume of a cubic micron.

III. EXCIMER LASER IRRADIATION EFFECTS IN $Fe_{66}Co_{18}B_{15}Si$ AMORPHOUS SYSTEM

Room-temperature transmission Mössbauer spectra of the $Fe_{66}Co_{18}B_{15}Si$ samples, in the amorphous as-quenched state and after pulsed-excimer-laser irradiation ($\lambda=308$ nm, $\tau=10$ ns) with 2, 5, and 10 laser pulses per spot at a laser fluence of 5×10^{18} photons/cm^2 and a repetition rate of 1 Hz, are shown in Figs. 1(a)–1(d). The broad absorption lines in the Möss-

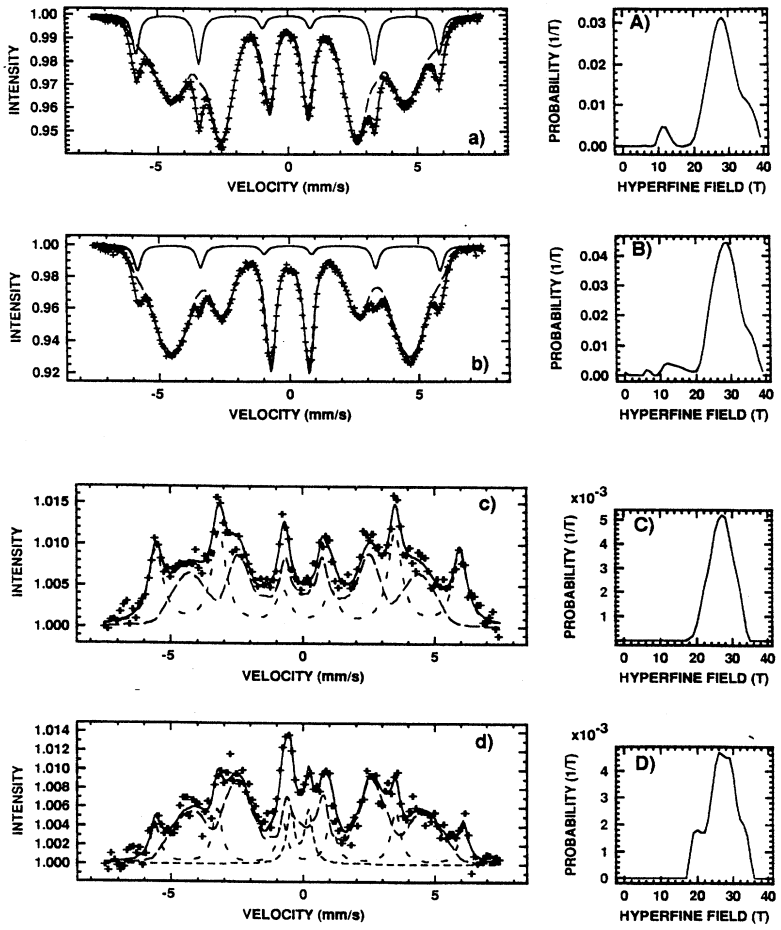

FIG. 2. Room-temperature Mössbauer spectra of the $Fe_{66}Co_{18}B_{15}Si$ samples, after thermal annealing at 648 K for 1 h and subsequent pulsed-excimer-laser irradiation: (a) transmission Mössbauer spectrum of thermally-annealed sample; (b) transmission Mössbauer spectrum of thermally annealed and excimer-laser-irradiated sample; (c) CEMS spectrum of thermally annealed sample; (d) CEMS spectrum of thermally annealed and excimer-laser-irradiated sample. The corresponding hyperfine magnetic field distributions extracted from the Mössbauer spectra are presented in (A)–(D).

bauer spectra are due to various nearest-neighbor configurations of the resonant atoms in the amorphous structure. The different inequivalent sites determine fluctuations of the hyperfine parameters, which are described in terms of the corresponding distributions. Figures 1(A)–1(D) show the hyperfine magnetic field distributions extracted from the transmission Mössbauer spectra. The fitted values of the hyperfine parameters corresponding to the as-quenched and pulsed-laser-treated $Fe_{66}Co_{18}B_{15}Si$ samples are listed in Table I.

For the 14.4 keV γ rays of ^{57}Fe, the relative intensity of the second (fifth) to the first (sixth) lines is given, in the thin absorber approximation, by[14]

$$R_{21}=4\ \sin^2\alpha/[3(1+\cos^2\alpha)], \quad (1)$$

where α is the angle between the γ-ray propagation direction and the direction of the net magnetic moment. The ratio R_{21} varies from 0 to 4/3 as α changes from 0° to 90° and for a completely random distribution of magnetic-moment directions, takes the value 0.67. It can be seen in Fig. 1(b), for the $Fe_{66}Co_{18}B_{15}Si$ sample irradiated with 2 laser pulses per spot, that laser-induced effects have resulted in a pronounced decrease of the intensity ratio of the second to the first line. The corresponding value of the magnetic texture parameter R_{21} (Table I) shows that a rotation of the average magnetic-moment direction from the in-plane to an out-of-plane orientation has taken place. For the $Fe_{66}Co_{18}B_{15}Si$ samples irradiated with 5 and 10 laser pulses per spot [Figs. 1(c) and 1(d), respectively], the areal intensity ratio R_{21} progressively increases as compared to the spectrum in Fig. 1(b), but remains different from the value indicating the random distribution of magnetic-moment directions. Consequently, the average direction of bulk magnetization in $Fe_{66}Co_{18}B_{15}Si$ maintains a preferred out-of-plane orientation upon increasing the number of applied pulses during excimer laser irradiation. This behavior is in qualitative agreement with the dependence of the intensity ratio R_{21} on the repetition rate, as determined by isochronal excimer laser annealing of iron-based and nickel-iron-based alloy samples.[9] The average hyperfine magnetic field $\langle H_{hf}\rangle$, width of the field distribution ΔH_{hf}, and total absorption area in the Mössbauer spectra (Table I) show no significant variations during the laser treatment performed, suggesting the absence of crystallization effects in the irradiated $Fe_{66}Co_{18}B_{15}Si$ samples. As in the case of laser-treated iron-based and nickel-iron-based metallic glasses,[8–11] it can be assumed that the high heating and cooling rates associated with pulsed laser irradiation determined the formation of compressive stresses in the surface and tensile stresses in the bulk. Since it has been shown that in magnetic specimens, due to magnetoelastic effects, internal stresses generated by surface modifications may dramatically change the bulk magnetic properties,[15] the out-of-plane reorientation of the average magnetization direction observed in the present irradiation study gives further support to the formation of closure domain structure[8,9] in the laser treated samples. Moreover, these results show that the direction of bulk magnetization in the $Fe_{66}Co_{18}B_{15}Si$ amorphous system can be controlled by appropriate selection of irradiation parameters.

IV. EXCIMER LASER IRRADIATION EFFECTS IN PARTIALLY CRYSTALLIZED $Fe_{66}Co_{18}B_{15}Si$ SYSTEM

In order to gain additional information on the fundamental effects underlying the interaction of laser radiation with glassy ferromagnets, the present study further investigates the influence of pulsed-laser treatment on the magnetic and structural properties of thermally annealed $Fe_{66}Co_{18}B_{15}Si$ samples.

Figure 2(a) shows the room-temperature transmission Mössbauer spectrum of the $Fe_{66}Co_{18}B_{15}Si$ sample, after thermal annealing at 648 K for 1 h. The sharp six-line pattern in the Mössbauer spectrum exhibits a hyperfine magnetic splitting of 362.1 kOe and corresponds to the α-(FeCo) crystal-

TABLE II. Hyperfine magnetic field H_{hf}, isomer shift δ (relative to α-Fe at 300 K), quadrupole splitting ΔE_Q, intensity ratio R_{21}, and relative areas corresponding to component patterns in the transmission and conversion electron Mössbauer spectra of $Fe_{66}Co_{18}B_{15}Si$ samples, thermally annealed at 648 K for 1 h and excimer laser irradiated.

Treatment of samples	Type of data	Subsp. no.	H_{hf} (kOe)	δ (mm/s)	ΔE_Q (mm/s)	R_{21}	Relative areas (%)	Assignment of phases
	Bulk	I	362.1	0.04		1.25	11.5	α-(FeCo)
		II	279.3	0.03		0.95	88.5	Amorphous
Thermally annealed	Surface	I	356.9	0.05		0.92	46.1	α-(FeCo)
		II	231.7	0.04		0.78	53.9	Amorphous
	Bulk	I	360.9	0.05		0.88	7.1	α-(FeCo)
Thermally annealed		II	278.9	0.02		0.36	92.9	Amorphous
and laser	Surface	I	362.0	0.04		0.41	24.2	α-(FeCo)
irradiated		II		0.15	0.78	1.00	7.3	FeO
		III	242.1	0.04		0.99	68.5	Amorphous
Errors:			±1.5	±0.015	±0.02	±0.02	±1.0	

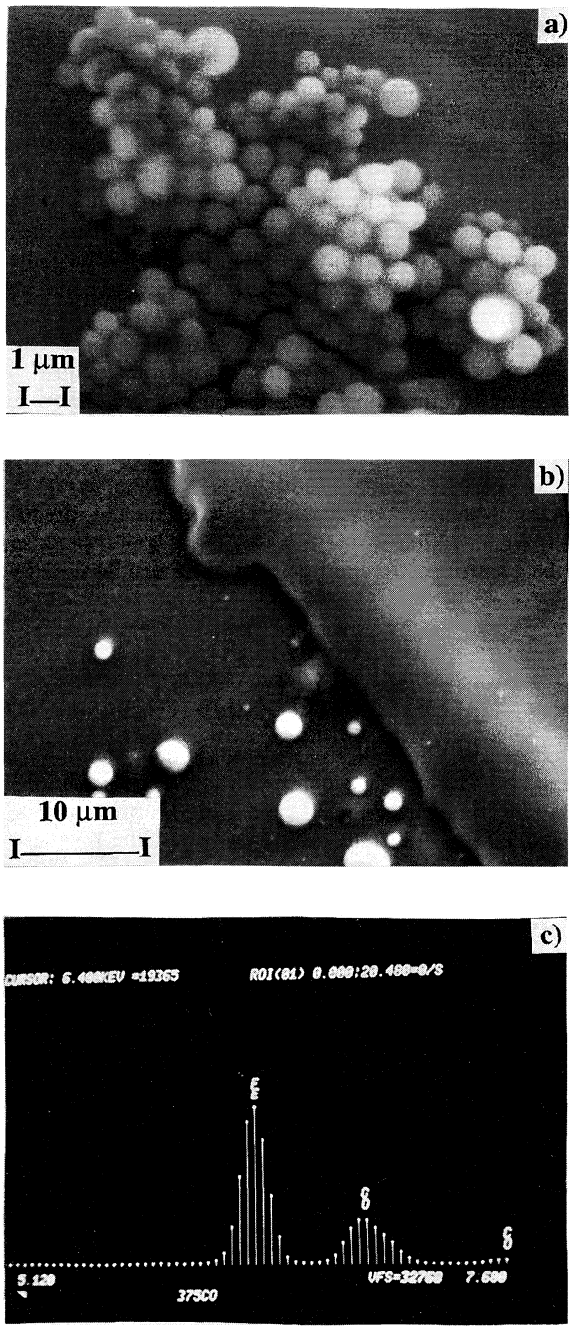

FIG. 3. (a) SEM micrograph of the $Fe_{66}Co_{18}B_{15}Si$ sample, after thermal annealing at 648 K for 1 h; (b) SEM examination of the $Fe_{66}Co_{18}B_{15}Si$ sample, after thermal annealing at 648 K for 1 h and subsequent pulsed-excimer-laser irradiation ($\lambda=308$ nm, $\tau=10$ ns, $\Phi_L=5\times10^{18}$ photons/cm^2, repetition rate 1 Hz); (c) EDX analysis of the crystalline precipitates observed in the SEM photograph of the thermally annealed $Fe_{66}Co_{18}B_{15}Si$ sample.

line phase. This result is in agreement with the previous identification of α-(FeCo) in the primary crystallization process of $Fe_{78-x}Co_xSi_9B_{13}$ amorphous alloy, based on differential thermal analysis.[3] As indicated by the corresponding R_{21} values in Table II, the magnetic moments of the α-(FeCo) crystalline phase are preferentially oriented in the plane of the foil. The hyperfine magnetic field distribution shown in Fig. 2(A) corresponds to the remaining amorphous matrix. The partially crystallized sample was further exposed to pulsed-excimer-laser irradiation ($\Phi_L=5\times10^{18}$ photons/cm^2) with 2 laser pulses per spot at a repetition rate of 1 Hz. The room-temperature transmission Mössbauer spectrum and hyperfine magnetic field distribution of the irradiated $Fe_{66}Co_{18}B_{15}Si$ sample are shown in Figs. 2(b) and 2(B), respectively. It can be inferred from Table II that the α-(FeCo) content decreased from 11.5% in the thermally annealed system to 7.1% in the laser-exposed specimen. At the same time, a pronounced out-of-plane reorientation of the magnetic-moment directions resulted as an effect of the laser irradiation performed. Consequently, excimer-laser-induced revitrification was evidenced in the partially crystallized $Fe_{66}Co_{18}B_{15}Si$ system and was found to be accompanied by the development of laser-induced magnetic anisotropy.

In order to obtain a complete characterization of the laser-induced phase transformation in $Fe_{66}Co_{18}B_{15}Si$ glassy ferromagnet, a separate surface analysis of the partially-crystallized and laser-irradiated specimens has been performed. Figures 2(c) and 2(d) show the conversion electron Mössbauer spectra of the $Fe_{66}Co_{18}B_{15}Si$ samples, after thermal annealing at 648 K and subsequent pulsed-excimer-laser treatment. The hyperfine magnetic field distributions extracted from these spectra are given in Figs. 2(C) and 2(D), respectively. It can be observed in Table II that the α-(FeCo) content of the 100 nm thick surface layer probed decreased from 46.1% in the partially crystallized system to 24.2% in the laser-exposed specimen. As indicated by the corresponding R_{21} values, the magnetic-moment directions in the upper surface layer exhibit a preferred in-plane orientation, similar to that observed for the as-quenched ribbon. When compared to bulk measurements, this result demonstrates a different behavior of the surface magnetic texture upon irradiation, suggesting the occurrence of a distribution of magnetic-moment directions through the thickness of the foil.[9] In addition to the six-line pattern corresponding to the α-(FeCo) crystalline phase and the magnetic field distribution associated with the remaining amorphous matrix, CEMS analysis reveals the presence of a quadrupole-split doublet in the spectrum of the laser-irradiated sample, which has been assigned to nonstoichiometric iron oxides.[9,15] Indeed, an oxidation mechanism of Fe^0 to Fe^{2+}, which initially leads to precipitation of FeO particles, can be assumed.[16] Consequently, the nature of the laser-induced phase transformation in partially crystallized $Fe_{66}Co_{18}B_{15}Si$ specimens was elucidated and found to consist of partial amorphization and surface oxidation of the irradiated material. One may note that the effect of excimer-laser-induced crystallization, recently observed[9] in a $Fe_{77}Cr_2B_{16}Si_5$ amorphous alloy at high repetition rates and laser fluences, was also shown to be accompanied by the precipitation of FeO particles on the irradiated surface.

Distinctive features regarding the laser-induced surface modifications can be observed in the SEM examinations of the $Fe_{66}Co_{18}B_{15}Si$ sample (Fig. 3). These investigations demonstrate the presence of crystalline precipitates on the surface of the $Fe_{66}Co_{18}B_{15}Si$ sample annealed at 648 K for 1 h [Fig. 3(a)]. The nature of these surface precipitates was identified

by EDX analysis of the corresponding microvolumes [Fig. 3(c)], which supported the Mössbauer spectroscopy observation of the α-(FeCo) phase as the first crystalline product in $Fe_{66}Co_{18}B_{15}Si$ amorphous alloy. SEM examinations of the partially crystallized $Fe_{66}Co_{18}B_{15}Si$ system, after pulsed-excimer-laser irradiation ($w=3$ J/cm^2) with 2 laser pulses per spot at a repetition rate of 1 Hz were also performed [Fig. 3(b)]. One may note that the single pulse energy density employed was above the reported threshold of ~ 2 J/cm^2 for the ablation of transition metals.[17] Correspondingly, the SEM micrograph reveals intriguing features in the region of laser-pulse incidence on the surface of the thermally annealed alloy sample (right side of the micrograph). The uniform aspect of the laser-irradiated area is indicative of amorphous phase formation, due to laser-induced melting and rapid solidification. This demonstrates that the laser treatment performed resulted in redissolution of most precipitate particles. The molten zones which subsequently resolidified following pulsed-laser irradiation give rise to complex internal stresses, which are responsible for the observed out-of-plane reorientation of the bulk magnetization direction. An additional morphological feature observable in the SEM micrograph of Fig. 3(b) is represented by the formation of droplets on the laser-irradiated surface. This effect is attributed to laser-induced shock waves,[9,18,19] which determine boiling of the metal surface and plasma production, due to a dramatic increase in the surface temperature and a simultaneous decrease in the metal's reflectivity. Expulsion of droplets from the laser-induced melt on the irradiated surface demonstrates an enhanced momentum transfer from plasma to target material,[20] due to the recoil pressure of the breakdown plasma expansion. On these grounds, it can be inferred that ablation pressures are high enough to change interatomic distances and cause revitrification of the laser-irradiated material.

V. EXCIMER LASER IRRADIATION EFFECTS IN TOTALLY CRYSTALLIZED $Fe_{66}Co_{18}B_{15}Si$ SYSTEM

Aiming at a complete characterization of the effects associated with the interaction of pulsed laser radiation with Fe-Co based metallic glasses, in this section we present investigations of the influence of excimer laser treatment on the phase composition and magnetic behavior of totally crystallized $Fe_{66}Co_{18}B_{15}Si$ samples.

Figure 4(a) shows the room-temperature transmission Mössbauer spectrum of the $Fe_{66}Co_{18}B_{15}Si$ sample, after thermal annealing at 723 K for 1 h. The spectrum was analyzed considering two six-line patterns, corresponding to the α-(FeCo) and $(FeCo)_3(BSi)$ crystalline phases. The relative abundance of crystalline phases (Table III) is different for the upper 100 nm surface layer. Moreover, an additional crystalline phase, identified as $(FeCo)_2(BSi)$ was revealed by CEMS spectrum analysis [Fig. 4(c)]. The phase identification results obtained in the present study are in good agreement with the crystalline phase formation observed by radio frequency annealing of $Fe_xCo_{78-x}Si_9B_{13}$ amorphous alloy.[6] The totally crystallized $Fe_{66}Co_{18}B_{15}Si$ sample was further exposed to pulsed-excimer-laser irradiation ($\Phi_L=5\times10^{18}$ photons/cm^2) with 2 laser pulses per spot at a repetition rate of 1 Hz. The room-temperature transmission and conversion electron Mössbauer spectra of the irradiated $Fe_{66}Co_{18}B_{15}Si$ specimen are shown in Figs. 4(b) and 4(d), respectively. It can be observed in Table III that the bulk α-(FeCo) content decreased from 66.3% in the completely crystallized sample to 30.3% in the laser-exposed specimen. The most interesting result obtained from phase analysis of the laser-irradiated $Fe_{66}Co_{18}B_{15}Si$ system, however, is the absence of the $(FeCo)_3(BSi)$ crystalline component, formed in the second stage of the crystallization process by thermal annealing. Instead, the balance of the composition is represented by an amorphous phase, in which a pronounced out-of-plane reorientation of the magnetic-moment directions re-

TABLE III. Hyperfine magnetic field H_{hf}, isomer shift δ (relative to α-Fe at 300 K), quadrupole splitting ΔE_Q, intensity ratio R_{21}, and relative areas corresponding to component patterns in the transmission and conversion electron Mössbauer spectra of $Fe_{66}Co_{18}B_{15}Si$ samples, thermally annealed at 723 K for 1 h and excimer laser irradiated.

Treatment of samples	Type of data	Subsp. no.	H_{hf} (kOe)	δ (mm/s)	ΔE_Q (mm/s)	R_{21}	Relative areas (%)	Assignment of phases
	Bulk	I	360.5	0.05		0.54	66.3	α-(FeCo)
		II	232.5	0.09		0.84	33.7	$(FeCo)_3(BSi)$
Thermally annealed	Surface	I	362.9	0.05		0.83	53.8	α-(FeCo)
		II	295.9	0.11		0.83	24.7	$(FeCo)_2(BSi)$
		III	219.9	0.08		0.83	21.5	$(FeCo)_3(BSi)$
	Bulk	I	361.8	0.06		0.35	30.3	α-(FeCo)
Thermally annealed		II	275.0	0.04		0.41	69.7	Amorphous
and laser	Surface	I	359.1	0.05		0.48	30.3	α-(FeCo)
irradiated		II		0.15	0.78	1.00	6.1	FeO
		III	208.1	0.03		0.16	63.6	Amorphous
Errors:			±1.5	±0.015	±0.02	±0.02	±1.0	

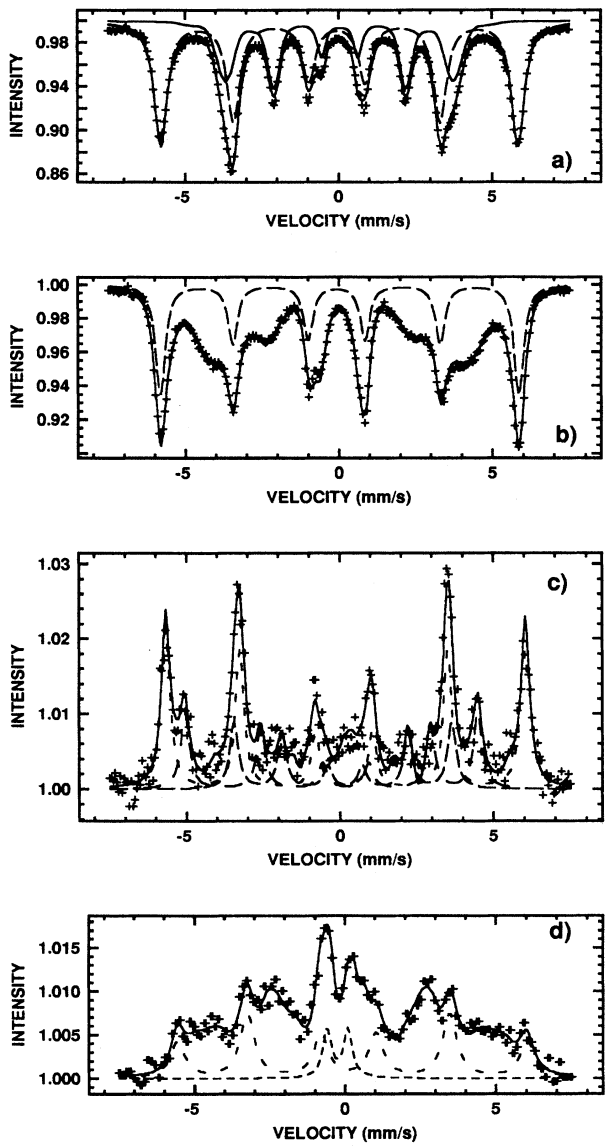

FIG. 4. Room-temperature Mössbauer spectra of the $Fe_{66}Co_{18}B_{15}Si$ samples, after thermal annealing at 723 K for 1 h and subsequent pulsed-excimer-laser irradiation: (a) transmission Mössbauer spectrum of thermally annealed sample; (b) transmission Mössbauer spectrum of thermally annealed and excimer-laser-irradiated sample; (c) CEMS spectrum of thermally annealed sample; (d) CEMS spectrum of thermally annealed and excimer-laser-irradiated sample.

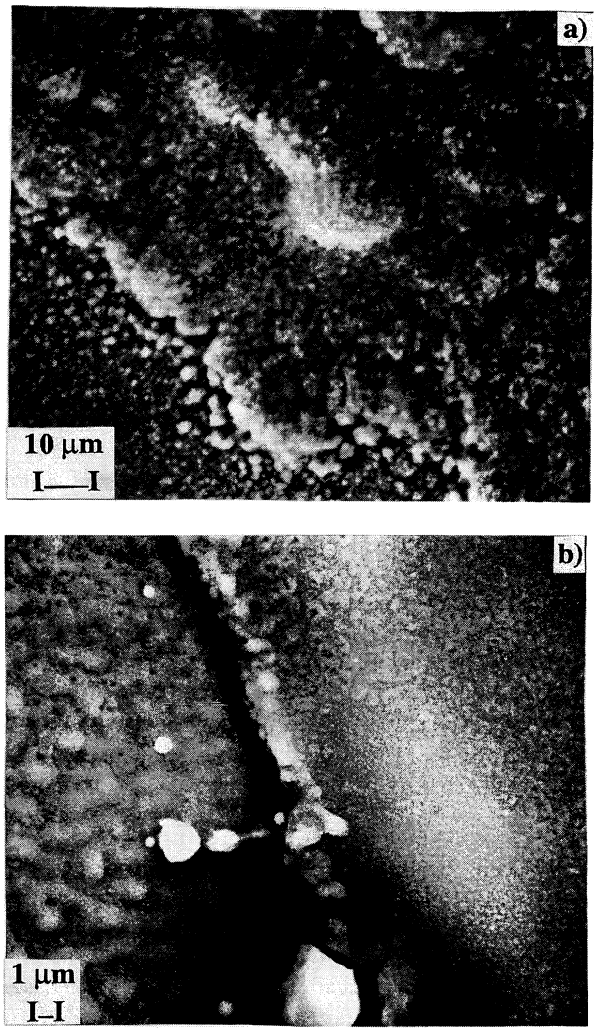

FIG. 5. SEM micrographs of the $Fe_{66}Co_{18}B_{15}Si$ sample: (a) after thermal annealing at 723 K for 1 h; (b) after thermal annealing and excimer laser irradiation ($\lambda=308$ nm, $\tau=10$ ns, $\Phi_L=5\times10^{18}$ photons/cm^2, repetition rate 1 Hz).

sulted as an effect of the laser irradiation performed. Consequently, the present study shows that the effect of excimer-laser-induced amorphization in totally crystallized $Fe_{66}Co_{18}B_{15}Si$ system exhibits phase selectivity with respect to the crystalline components of the ferromagnetic alloy. As in the case of partially crystallized $Fe_{66}Co_{18}B_{15}Si$ system, the laser-induced amorphization was found to be accompanied by the development of an out-of-plane magnetic anisotropy.

The morphology of the crystallized phases formed in the thermally annealed $Fe_{66}Co_{18}B_{15}Si$ system and the characteristics of the laser-induced surface modifications in the totally crystallized specimen can be observed in the SEM micrographs of Figs. 5(a) and 5(b), respectively. The amorphization process originates in the molten zones subsequently quenched due to pulsed-excimer-laser irradiation, while the mechanical stresses associated with rapid heating and cooling are suggested to be responsible for the reorientation of the easy magnetization axis.

CEMS surface analysis of the totally crystallized laser-irradiated $Fe_{66}Co_{18}B_{15}Si$ system [Fig. 4(d)] supports the bulk Mössbauer results: the $(FeCo)_3(BSi)$ and $(FeCo)_2(BSi)$ crystalline phases are absent, due to excimer-laser-induced amorphization, from the composition of the irradiated specimen. In the upper surface layer, the relative abundance of the stable α-(FeCo) crystalline phase, formed in the primary crystallization process of the $Fe_{66}Co_{18}B_{15}Si$ alloy, decreased from 53.8% in the completely crystallized sample to 30.3% in the laser-exposed specimen. In addition to the dominant amorphous component, CEMS analysis reveals the presence

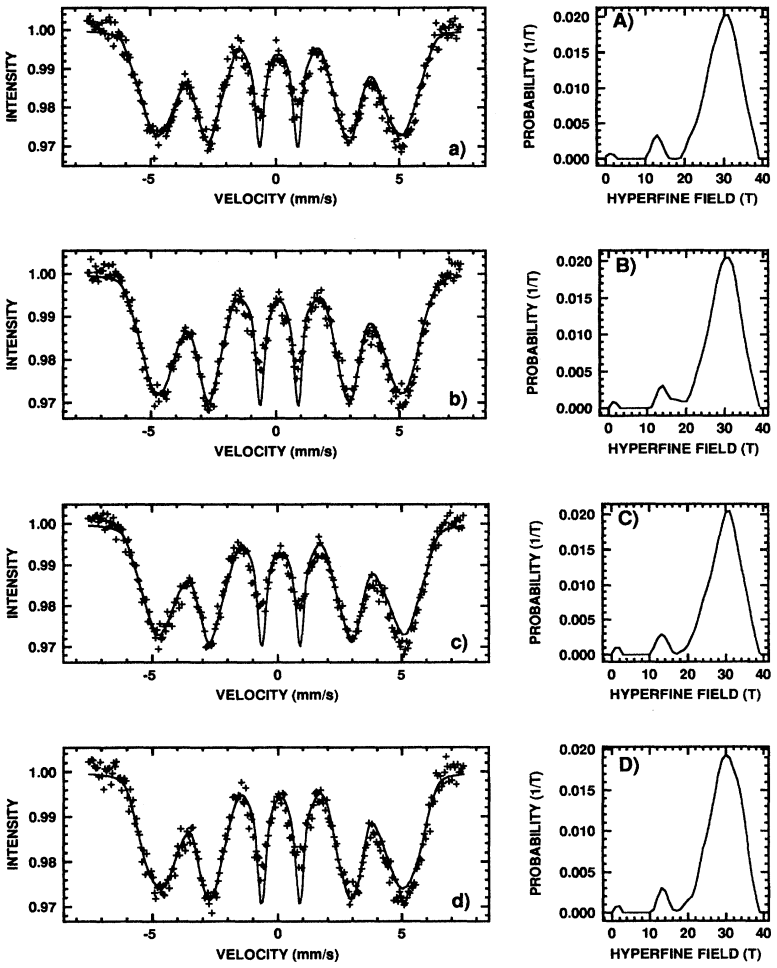

FIG. 6. Low-temperature transmission Mössbauer spectra of the $Fe_{66}Co_{18}B_{15}Si$ as-quenched amorphous: (a) $T=15$ K; (b) $T=35$ K; (c) $T=55$ K; (d) $T=70$ K. The corresponding hyperfine magnetic field distributions are shown in (A–D).

of the quadrupole-split doublet corresponding to FeO particles.

Consequently, the nature of the laser-induced phase transformation in totally crystallized $Fe_{66}Co_{18}B_{15}Si$ specimens is found to consist of partial amorphization and surface oxidation of the irradiated material. Although the present laser irradiation treatment was carried out in air, it would be interesting to further investigate the effect of various ambient atmospheres on the laser-induced phase transformations in metallic glasses. Excimer-laser-induced revitrification was found to exhibit selectivity with regard to the component crystalline phases in the $Fe_{66}Co_{18}B_{15}Si$ annealed system and was accompanied by laser-induced reorientation of the average bulk magnetization direction. The present results suggest that excimer laser irradiation of glassy ferromagnets promotes selective control over important structural and magnetic characteristics of the material, which has not been achieved using conventional processing methods.

VI. LOW-TEMPERATURE MAGNETIC BEHAVIOR OF AMORPHOUS AND EXCIMER-LASER IRRADIATED $Fe_{66}Co_{18}B_{15}Si$ SYSTEM

The investigations described in this section were performed in order to determine the temperature dependence of the average hyperfine magnetic field of amorphous and laser-irradiated $Fe_{66}Co_{18}B_{15}Si$ system. Typical Mössbauer spectra of $Fe_{66}Co_{18}B_{15}Si$ amorphous alloy at low temperatures are shown in Fig. 6, along with the corresponding hyperfine magnetic field distributions. In contradistinction to the preferred in-plane orientation of the average magnetization direction at room temperature, Mössbauer spectra analysis ($R_{21}=0.66$) indicated that the magnetization axis of the $Fe_{66}Co_{18}B_{15}Si$ as-quenched sample was altered to more random directions at low temperatures (15–70 K). It should be mentioned that the $Fe_{66}Co_{18}B_{15}Si$ sample studied was not subjected to any stresses, except for those inherent to the cooling process from room temperature to the temperature of measurement. Similar investigations were performed for the $Fe_{66}Co_{18}B_{15}Si$ amorphous alloy irradiated with 2 laser pulses per spot. The temperature dependence of the hyperfine magnetic field of amorphous and excimer-laser-irradiated $Fe_{66}Co_{18}B_{15}Si$ system is shown in Fig. 7(a). Figure 7(b) presents the fractional change of hyperfine field as a function of $(T/T_C)^{3/2}$ for both amorphous and irradiated specimens. For amorphous ferromagnets, the magnetic hyperfine field decreases with increasing temperature according to[21]

$$[H_{hf}(T)-H_{hf}(0)]/H_{hf}(0)=-B_{3/2}(T/T_C)^{3/2}. \quad (2)$$

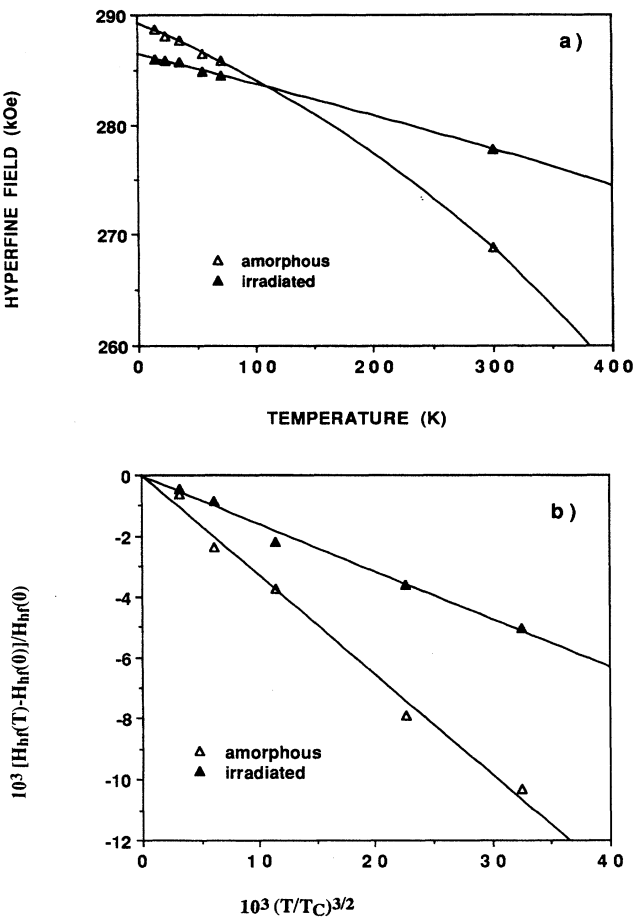

FIG. 7. (a) Temperature dependence of the magnetic hyperfine field of as-quenched amorphous and pulsed-excimer-laser irradiated $Fe_{66}Co_{18}B_{15}Si$ alloy; (b) fractional change of hyperfine field versus $(T/T_C)^{3/2}$ for amorphous and irradiated $Fe_{66}Co_{18}B_{15}Si$. The solid line is the result of least-squares fit of the data points.

This temperature dependence originates in the excitations of long-wavelength spin waves, for which detailed atomic arrangements are not important. A least-squares fit of Eq. (2) to the magnetic hyperfine field data gave $B_{3/2}=0.32\pm0.05$, value which is much larger than those obtained for crystalline ferromagnets (for example, $B_{3/2}=0.12$ for α-Fe). Moreover, the temperature coefficient of the $Fe_{66}Co_{18}B_{15}Si$ amorphous specimen is twice that obtained for the laser-irradiated system ($B_{3/2}=0.16\pm0.03$).

Magnetization and Mössbauer spectroscopy measurements in several glassy ferromagnets[21] show that the measured hyperfine field $H_{\rm eff}(T)$ and the magnetization $M(T)$ are proportional. Thus the temperature dependence of the reduced hyperfine field reflects the temperature dependence of the reduced magnetization. Several theoretical calculations of the magnetization of noncrystalline ferromagnets considered a random fluctuation of the exchange constants in the Heisenberg interaction and used the molecular field approximation. Thus the reduced magnetization of a glassy ferromagnet has the form[22]

$$\sigma=M(T)/M(0)=(1/2)\{B_S[(1+\delta)x]+B_S[(1-\delta)x]\}, \tag{3}$$

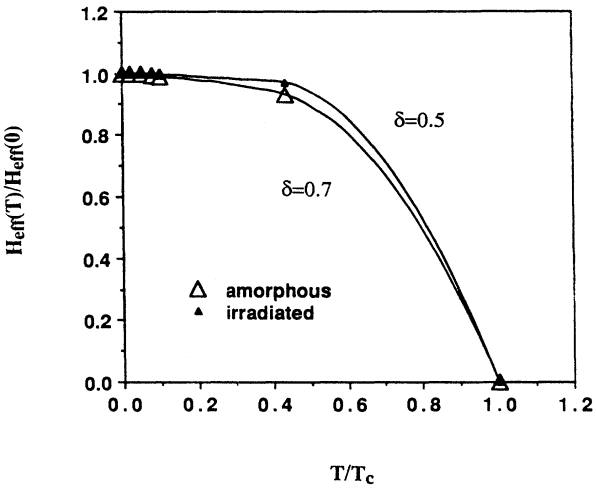

FIG. 8. Reduced hyperfine field as a function of reduced temperature for amorphous and laser-irradiated $Fe_{66}Co_{18}B_{15}Si$. The solid curves are computer plots of Eq. (3).

with

$$x=3S(S+1)T_C\sigma/T. \tag{4}$$

Here B_S is the Brillouin function for spin S, T_C is the Curie temperature, and $0<\delta<1$ is the root-mean-square fluctuation of the exchange constant in the Heisenberg interaction. Equation (3) retains the well-known form for crystalline ferromagnets[23] by setting $\delta=0$:

$$\sigma=B_S(x). \tag{5}$$

These relations make it possible to compare the experimental data with the calculated results in order to estimate the value of δ. On these grounds, we find that the experimental curve corresponding to the $Fe_{66}Co_{18}B_{15}Si$ amorphous ferromagnet approached the theoretical one for $\delta=0.7$, while the value $\delta=0.5$ was closest for the laser-treated alloy (see Fig. 8). These results show that excimer-laser-irradiation reduces the fluctuations of exchange interactions in the $Fe_{66}Co_{18}B_{15}Si$ ferromagnetic system, due to laser-induced quenching stresses. The conclusion supports similar findings of decreased fluctuations in the exchange interactions and free volume of a heat-treated $Fe_{81}B_{13.5}Si_{3.5}C_2$ metallic glass.[22]

VII. CONCLUSIONS

The main results obtained in the present study can be summarized as follows.

(i) In addition to inducing controlled magnetic anisotropy in the $Fe_{66}Co_{18}B_{15}Si$ amorphous system, pulsed-excimer-laser irradiation was shown to cause revitrification of partially crystallized $Fe_{66}Co_{18}B_{15}Si$ samples. The effect of excimer-laser-induced amorphization was found to be accompanied by changes in the bulk magnetization direction.

(ii) In totally crystallized $Fe_{66}Co_{18}B_{15}Si$ specimens, laser-induced partial amorphization was shown to exhibit phase selectivity relative to the crystalline components in the alloy system. Differences between surface and bulk behavior of the magnetic texture and phase composition were observed.

(iii) Low-temperature studies showed that laser-induced quenching stresses prevented the fluctuations of exchange interactions in the excimer-laser-irradiated $Fe_{66}Co_{18}B_{15}Si$ sample.

(iv) Excimer laser irradiation of glassy ferromagnets offers the intriguing opportunity of obtaining hybrid materials with select structural and magnetic characteristics.

ACKNOWLEDGMENTS

This work has been supported by the National Science Foundation and the Office of Naval Research.

*Permanent address.

[1] I. Turek, J. Kudrnovsky, V. Drchal, and P. Weinberg, Phys. Rev. B **49**, 3352 (1994).

[2] H. H. Hamdeh, B. Fultz, and D. H. Pearson, Phys. Rev. B **39**, 11 233 (1989).

[3] G. A. Stergioudis, J. Yankinthos, P. J. Rentzeperis, Z. Bojarski, and T. J. Panek, J. Mater. Sci. **27**, 2468 (1992).

[4] M. L. Fdez-Gubieda, J. M. Barandiaran, and F. Plazaola, J. Magn. Magn. Mater. **104-107**, 82 (1992).

[5] M. D. Baro, S. Surinach, J. A. Diego, and M. T. Clavaguera-Mora, Mater. Sci. Eng. A **135**, 807 (1991).

[6] M. Kopcewicz, M. El Zayat, and U. Gonser, J. Magn. Magn. Mater. **72**, 119 (1988).

[7] J. Sitek, M. Miglierini, J. Lipka, P. Valko, and I. Toth, Hyperfine Interact. **60**, 777 (1990).

[8] M. Sorescu and E. T. Knobbe, J. Mater. Res. **8**, 3078 (1993).

[9] M. Sorescu and E. T. Knobbe, Phys. Rev. B **49**, 3253 (1994).

[10] M. Sorescu, E. T. Knobbe, and D. Barb, Phys. Rev. B **51**, 840 (1995).

[11] M. Sorescu, E. T. Knobbe, and D. Barb, J. Phys. Chem. Solids **56**, 79 (1995).

[12] J. J. Spijkerman, in *Mössbauer Effect Methodology*, edited by I. J. Gruverman (Plenum, New York, 1971), Vol. 7, p. 85.

[13] R. A. Brand, J. Lauer, and D. M. Herlach, J. Phys. F **13**, 675 (1983).

[14] T. E. Cranshaw and G. Longworth, in *Mössbauer Spectroscopy Applied to Inorganic Chemistry*, edited by G. J. Long (Plenum, New York, 1984), Vol. 1, p. 173.

[15] M. Rogalski and I. Bibicu, Mater. Lett. **13**, 32 (1992).

[16] W. Meisel, J. Phys. (Paris) Colloq. Suppl. **41**, C1-63 (1980).

[17] J. C. S. Kools, in *Pulsed Laser Deposition of Thin Films,* edited by D. B. Chrisey and G. K. Hubler (Wiley, New York, 1994), p. 456.

[18] A. P. Radlinski, A. Calka, and B. Luther-Davies, Phys. Rev. Lett. **57**, 3081 (1986).

[19] C. Thomsen, H. T. Grahn, H. J. Maris, and J. Tauc, Phys. Rev. B **34**, 4129 (1986).

[20] J. Hermann, C. Boulmer-Leborgne, B. Debreuil, and I. N. Mihailescu, J. Appl. Phys. **74**, 3071 (1993).

[21] C. L. Chien and R. Hasegawa, Phys. Rev. B **16**, 3024 (1977).

[22] L. Lanotte, A. Annunziata, P. Silvestrini, and V. Tagliaferri, Nuovo Cimento **13D**, 1123 (1991).

[23] C. Kittel, *Introduction to Solid State Physics* (Wiley, New York, 1986), p. 428.

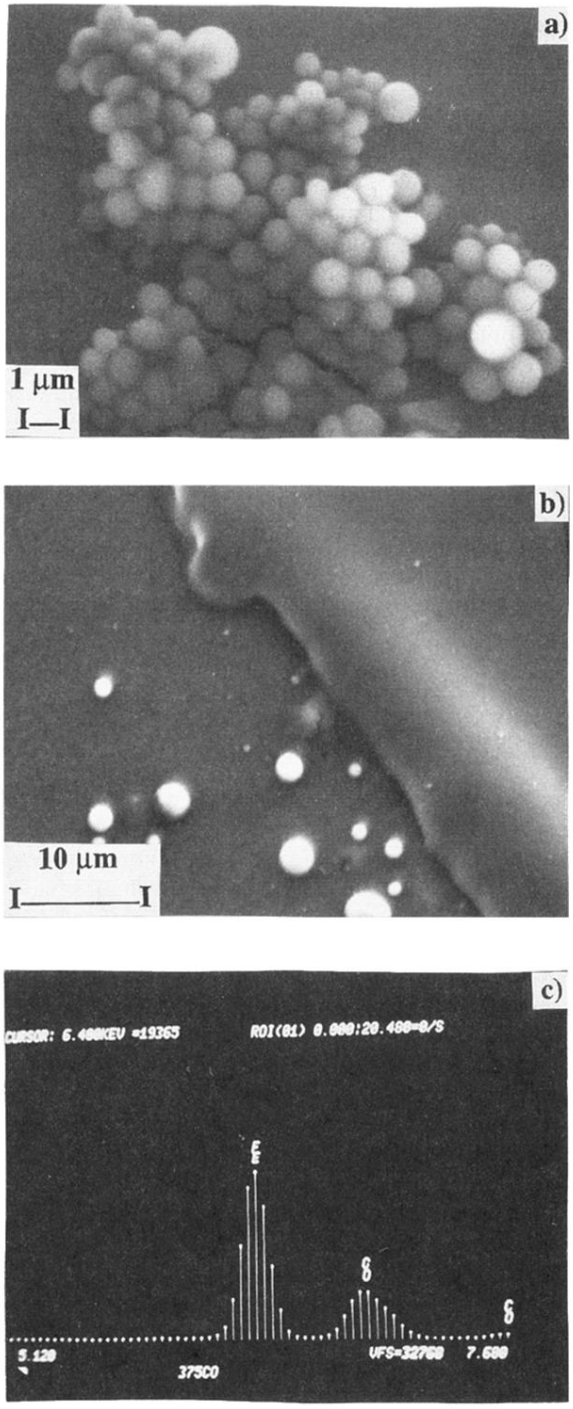

FIG. 3. (a) SEM micrograph of the $Fe_{66}Co_{18}B_{15}Si$ sample, after thermal annealing at 648 K for 1 h; (b) SEM examination of the $Fe_{66}Co_{18}B_{15}Si$ sample, after thermal annealing at 648 K for 1 h and subsequent pulsed-excimer-laser irradiation ($\lambda=308$ nm, $\tau=10$ ns, $\Phi_L=5\times10^{18}$ photons/cm^2, repetition rate 1 Hz); (c) EDX analysis of the crystalline precipitates observed in the SEM photograph of the thermally annealed $Fe_{66}Co_{18}B_{15}Si$ sample.

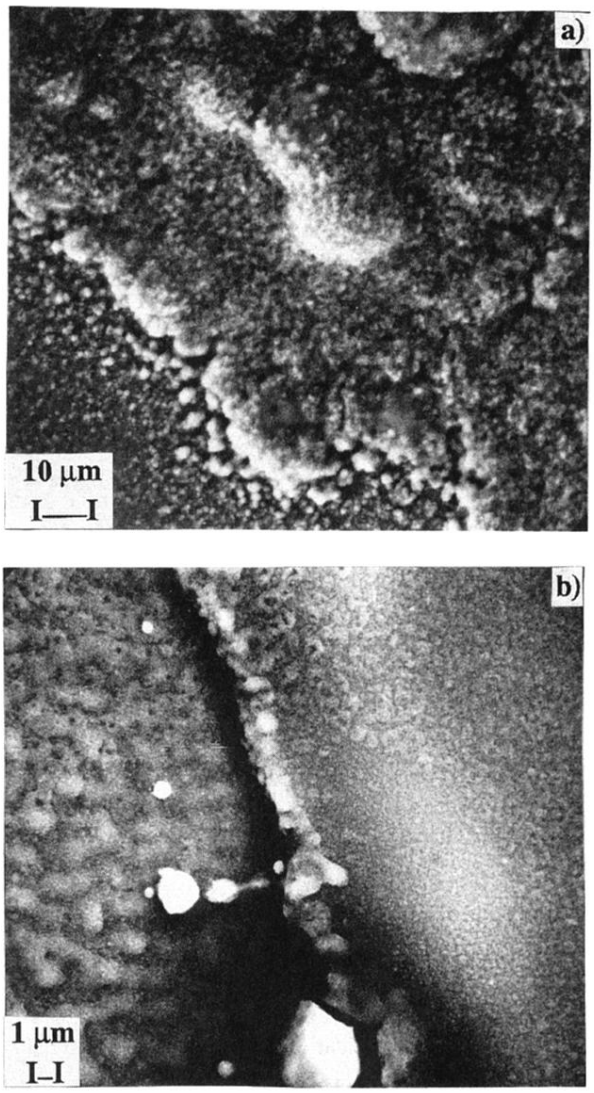

FIG. 5. SEM micrographs of the $Fe_{66}Co_{18}B_{15}Si$ sample: (a) after thermal annealing at 723 K for 1 h; (b) after thermal annealing and excimer laser irradiation ($\lambda=308$ nm, $\tau=10$ ns, $\Phi_L=5\times10^{18}$ photons/cm^2, repetition rate 1 Hz).